TECHNICAL TRANSACTIONS 4/2017
CZASOPISMO TECHNICZNE 4/2017
MECHANICS
DOI: 10.4467/2353737XCT.17.057.6368

Roman Dyga (r.dyga@po.opole.pl)
Department of Chemical and Process Engineering, Faculty of Mechanical Engineering, Opole University of Technology

Metal foams as structural packing in the construction of process equipment

Piany metalowe jako wypełnienia strukturalne w budowie aparatury przemysłowej

Abstract

The paper presents possibilities of the application of open-cell metal foams in the construction of process equipment. The article also describes results of own experimental studies on hydrodynamic and thermal phenomena occurring during fluid flow through channels packed with aluminium alloy foams. The collected experimental data enabled to determine, among others, pressure drops and the heat transfer coefficient, and to indicate main gas–liquid flow patterns.

Keywords: open-cell aluminium foam, gas–liquid flow, pressure drop, flow pattern, heat transfer

Streszczenie

W artykule przedstawiono możliwości wykorzystania otwartokomórkowych pian metalowych w budowie aparatury przemysłowej. Opisano wyniki własnych badań doświadczalnych dotyczących zjawisk hydrodynamicznych i cieplnych zachodzących podczas przepływu płynu przez kanały wypełnione pianami ze stopów aluminium. Zebrane dane eksperymentalne pozwoliły określić m.in. wartości oporów przepływu i współczynnika wnikania ciepła oraz wskazać podstawowe struktury przepływu gaz–ciecz.

Słowa kluczowe: otwartokomórkowa piana aluminiowa, przepływ gaz–ciecz, opory przepływu, struktury przepływu, wnikanie ciepła

1. Introduction

In the recent several years, there has been an increased interest in metal foams and their applications in the flow equipment. Open-cell metal foams are highly porous materials, in which metal has a form of a three-dimensional skeleton that forms relatively large and empty cells as adjacent polyhedral bodies. Such a structure gives the foams very high porosity, usually over 90%. High porosity and many "windows" joining individual cells allow fluid flow in the cellular space, which reduces energy costs of pumping the fluids through these materials. Moreover, open-cell foams have a high specific surface area, which in combination with low pressure drops makes them perceived more and more often as an alternative for other types of structural packing used in the construction of heat exchangers and mass exchangers. A relatively high thermal conductivity and a continuous skeleton structure that causes no heat resistance, which occurs at the interfaces of structural packing, makes foam applicable as specific fins on the external heat exchanging surface in thermal engineering. Technology allows for the production of foams from a wide spectrum of metal alloys. Foams are available that are made of materials that allow for their application in difficult working conditions, such as a high temperature or a chemically aggressive environment.

1.1. Metal foams in construction of process equipment

The literature presents information on the application of open-cell metal foam in the construction of compact heat-exchangers [3, 11], thermal storage [18, 20] and heat regenerators [2, 21], as well as chemical reactors [10, 19] including catalytic reactors [7, 13]. Moreover, foams can be used in evaporators of cooling equipment [6, 8] and solar collectors [22], as well as in column equipment [12, 15].

Studies on heat transfer in equipment filled with metal foams usually show significant (2 to 4 times) increase in the heat transfer coefficient in comparison with classic pipe and plate equipment not containing components increasing the heat transfer. According to Boomsm et al. [1] and Wang et al. [22], there may even be a 10-fold increase in the heat transfer coefficient. The authors of the paper [1] believe that an increased head transfer rate compensates increase in the demand of fluid pumping energy. As a result, heat exchangers with metal foams have greater heat transfer efficiency by up to 50% compared to plate heat exchangers. Metal foam heat exchangers also have a very good ratio of heat transfer rate to mass and volume of the exchanger. As reported by Ozmat et al. [11], it is possible to gain heat flux of up to 5000 kW/m^2.

As assessed by Youchison et al. [24], the structure of a foam skeleton provides relatively low pressure drops and a high heat transfer rate in comparison with sintered packed bed. Whereas Wang et al. [21] report better calorific effect of a foam exchanger in comparison with analogical equipment with copper mesh packing.

Quite different conclusions were drawn by the authors of the papers [14, 16]. Their studies involved a comparison of the heat transfer in tubular heat exchangers with heat transfer surface developed using metal foam and traditional fins. According to Sertkay et al. [16], the heat

transfer rate in the exchanger with intertubular spaces filled with metal foam is approx. 2 times lower than for lamellar fins. Similarly, Ribeiro and Barbosa [14] believe that exchangers with finned radiators have better thermohydraulic parameters.

Research works pay a lot of attention to foam applications in the flow boiling processes [6, 17]. Presence of foam temperature of the heating surface and shifts departure from nucleate boiling towards much higher heat flux [17, 23]. Hu et al. [6] report that heat transfer coefficient recorded during the flow of boiling coolant through a flat channel filled with metal foam is 1.5–2.6 higher than for boiling on flat surface (channel without packing). Even a higher difference (2–4 higher for the foam) occurs for boiling in pipes. At the same time, the authors of the paper [6] highlight the fact that presence of metal foam causes a significant increase in agent pressure drops, which contributes to a decrease in the cooling system efficiency.

An increase in heat transfer rate may be achieved using foam as packing of tubes of solar collectors. As stated by Wang et al. [22], the greater the heat transfer rate is as a result of flow disturbances in a boundary layer, the more intense the fluid mixing in the entire tube volume and an increased effective thermal conductivity due to foam in the pipe.

Available literature data indicate that despite an increasing number of research works, there are still difficulties in the determination of process effects obtained by the application of foams in the process equipment. There are numerous doubts or even contradictions regarding basic issues of heat transfers and flow hydrodynamic through cellular space of the foams. This is especially true for processes involving two-phase gas–liquid mixtures. So far, there has not been sufficient identification of the effect of flow conditions and foam geometrical parameters on pressure drops and changes in phase void fractions. There is no information on the flow pattern occurring during two-phase flow through metal foams and conditions of their formation.

Due to numerous gaps in knowledge, it was decided to conduct own experimental research on the effect of flow conditions, fluid properties and foam skeleton geometric parameters on the hydrodynamic and thermal phenomena in single- and two-phase gas–liquid flow through open-cell metal foams.

2. Scope and execution of experiments

The studies were conducted using three foams from aluminium alloys (Fig. 1) – two of AlSi7Mg alloy and one of Al 6101. The foams had similar porosity φ and a skeleton shape, but different geometric dimensions of the cells. Similarity of some foam parameters was necessary in order to clearly determine the effect of cell size on the thermal and flow processes occurring in the cellular space. Pore density was treated as a distinguishing factor of individual foams, which according to the foam manufacturers, was 20 and 30 PPI for AlSi7Mg foams and 40 PPI for Al 6101 foam. For metal foams, a term pore is used to indicate the "window" connecting adjacent cells (Fig. 1d). Pore and cell sizes were determined graphically based on microscopic image analysis of the foam skeleton. The images were taken at a 15x zoom with a scanning microscope. Per suggestions of the authors of the paper [9], equivalent diameter

was taken a cell size d_c of value equal to diameter of the circle of circumference equal cell circumference. An equivalent diameter of the pore was defined analogically d_p. Equivalent values were determined as averages from measurements of over one hundred cells and pores. The selected foam parameters are summarised in Table 1.

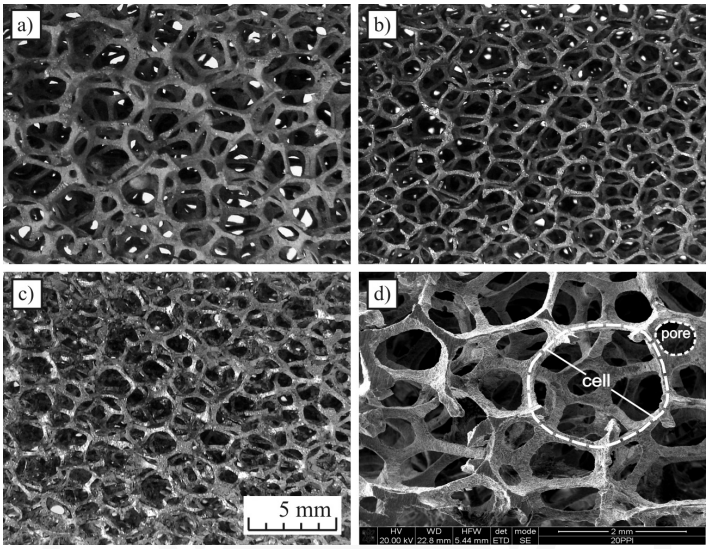

Fig. 1. Foams used in experiments: a) foam 20 PPI, b) foam 30 PPI, c) foam 40 PPI, d) microscopic image

An immediate purpose of the experimental studies was to measure pressure drops and changes in the temperatures of the fluid pumped through a channel filled with foams. For two-phase flows, void fractions of phases were measured and flow patterns were identified. Air, water and machine oil Velol-9Q were used as working liquids. The most important in terms of research subject, oil properties at 20°C were: viscosity $\eta_{ol} = 0.0086$ Pa·s, density $\rho_{ol} = 859.8$ kg/m^3, specific heat $c_{ol} = 1848.8$ J/(kg·K), thermal conductivity $k_{ol} = 0.128$ W/(m·K).

Table 1. Specification of tested foams

Foam (alloy)	φ [–]	k_s [W/(m·K)]	$d_c \cdot 10^{-3}$ [m]	$d_p \cdot 10^{-3}$ [m]
20 PPI (AlSi7Mg)	0.9336	150.4	3.452	1.094
30 PPI (AlSi7Mg)	0.9435	189.4	2.255	0.712
40 PPI (Al 6101)	0.9292	189.4	2.386	0.824

The measurements were conducted using an experimental stand, of which the main component was a horizontal channel with an internal diameter of 0.02 m, fully packed with aluminium foams (for each type of foam an independent channel was made). In the central

part of the channel, there was a measurement section of 1.27 m in length, where pressure drops and changes in the temperatures of the fluids and the channel wall were measured. The measurement section was preceded by a flow stabilising section. Downstream of the measurement section, there was an outlet section made of plexiglass, which despite the presence of packing, allowed for the observations of two-phase flow patterns occurring in the channel. A measurement section of the channel was heated externally on the length of 1.18 m, using a resistance heater coiled around the channel. In the heated part of the channel, the metal foam was glued to the external surface of the channel using a thermally conductive epoxy-aluminium adhesive. The measurement section was insulated with mineral wool. A diagram of the test stand with the location of the measurement instruments is presented in Figure 2, while the real view of the measurement section is presented in Figure 3.

The test stand was supplied with air from a pneumatic unit. Water (demineralised) was pumped using a multi-stage impeller pump, while oil – gear pump. Fluid streams were measured using various types of flow-meters of a high accuracy class. For air stream, due to high pressure drops and related changes in the air density, mass flow metres were used.

The pressure drop was measured as the difference of pressures between channel points 1 m apart from each other. The measurements were conducted using a set of five piezoresistive differential pressure sensors with a total measurement range of 0–150.000 Pa. For the determination of the air density, excess pressure in the channel was also measured. Phase void fractions were measured using the so-called trapping method. At the same time, using pneumatically controlled diaphragm valves, the inlet and outlet of the measurement section were closed. The trapped in the channel liquid volume in relation to volume of channel measurement section corresponded to the liquid fraction in the gas–liquid mixture.

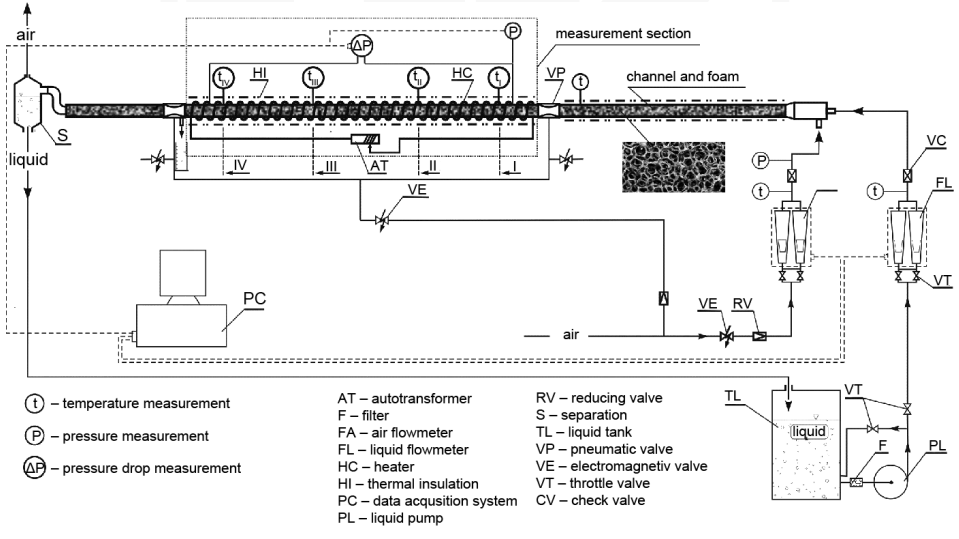

Fig. 2. Diagram of test stand

Temperatures of fluids and channel walls were measured using K-type thermocouples of 1 mm in diameter. Temperatures of the fluid and the wall were measured at four points along the channel (cross-section I, II, III and IV in Fig. 2). In each of the four cross-sections, 8 thermocouples were places. Measuring tips of five of them were inside the channel at different distances from its axis (in the vertical plane). Tips of three thermocouples were placed in the channel wall at distance of 0.5 mm from the internal channel surface.

The measurements were conducted for a relatively wide range of changes in the fluid velocities in order to obtain both laminar and turbulent flow. Fluids superficial velocity w_f was taken as a value characterising flow conditions. This velocity shall be understood as the average velocity of fluid through empty measurement channel neglecting the presence of the foam and a second fluid for a gas–liquid flow.

The measurements were conducted for adiabatic and nonadiabatic flow. In the latter case, the power of channel heating heaters was set at a level ensuring fluid temperature increase by at least 10 K.

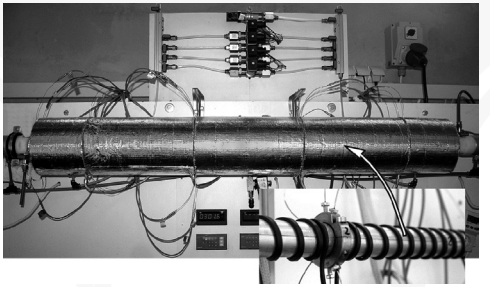

Fig. 3. Measurement section of test stand

Table 2. Experimental conditions

phase, f	w_f^* [m/s]	ζ_f [–]	t_f [°C]
air, *a*	0.028–9.88 (0.028–2.39)	0.313–0.998	21–95
water, *w*	0.003–0.270 (0.006–0.061)	0.002–0.988	24–88
oil, *ol*	0.003–0.167 (0.006–0.061)	0.002–0.988	19–93

* velocity range in brackets is for two-phase flow

3. Results of flow hydrodynamics and heat transfer

The measured single-phase flow pressure drops increase exponentially with the increase of fluid velocity. Figure 2 presents an example of such behaviour for pressure drops for water. For all three fluids, the lowest pressure drops were recorded for flow through foam 20 PPI, while

the greatest were observed for flow through foam 40 PPI. Foam 20 PPI has the largest cells, which makes it less resistant to flow than foams with smaller cells. Despite the fact that cell size of foam 40 PPI is slightly greater than for foam 30 PPI, pressure drops on foam 40 PPI are significantly higher than for flow through foam 30 PPI. This is due to the lower porosity and numerous local deformation of foam 40 PPI skeleton.

Pressure drop on tested foams can be described using Forchheimer equation,

$$\frac{\Delta P}{\Delta L} = \frac{\eta_f}{K} \cdot w_f + \rho_f \cdot \beta w_f^2, \tag{1}$$

where:

K – foam permeability, m^2,

β – foam inertial coefficient.

This equation is commonly used to describe flow through granular porous media, for which K and β are material specific constants. As shown in the paper [5], metal foams have various permeability and inertial coefficients, depending on the properties of fluids pumped through them. Due to this fact, applicability of the Forchheimer equation for fluid flow through metal foams is limited.

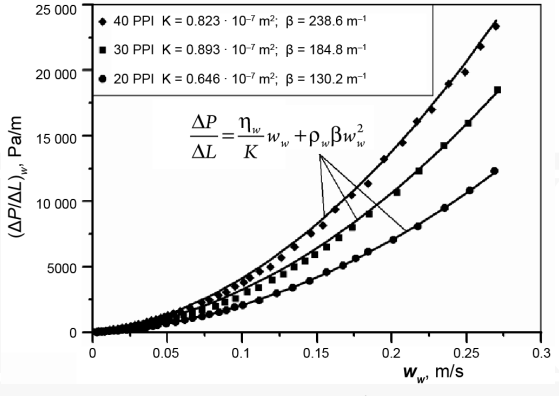

Fig. 4. Water pressure drop

A characteristic value for the single-phase through metal foams may be friction factor λ. It was concluded that this factor may be used as a generalised value that correctly describes the pressure drop on various foams, if its value is determined, allowing for geometric parameters of the foams. The value of the friction factor was determined based on the measured pressure drops and Darcy-Weisbach equation with hydraulic diameter d_h, adopted to be of equivalent value, determined based on two mutually independent parameters characterising foam geometry – porosity ϕ and pore diameter d_p,

$$d_h = \frac{\phi \cdot d_p}{1 - \varphi} \tag{2}$$

Analysis of change in the friction factor as a function of Reynolds number are given by the equation,

$$\mathrm{Re}_f = \frac{w_f \cdot d_h \cdot \rho_f}{\varphi \cdot \eta_f} \tag{3}$$

enables determination of nature of the flow through individual foams. Form low Reynolds number range, the friction factor decreases linearly (Fig. 5), which indicates that flow is laminar. For flow of both liquids, as well as for air, the flow is laminar when Re_f does not exceed a value of approx. 150. A clear departure of the curve of friction factor from linearity, when Re > 150, prove loss of flow stability and intensification of flow disturbances with increase in Re_f. It shall be noted that for Reynolds number below approx. 1300, a slope of the curve of changes in the friction factor is clearly greater than for Re > 1300. It may be assumed that for Re ≈ 150–1300 the flow has a transient Forchheimer nature. As indicated by the current state of knowledge, in the Forccheimer flow range, departures from the laminar flow are small. As the fluid velocity increases, the flow becomes more and more unstable and to a great extent exhibits features of the turbulent flow (Re_f > 1300).

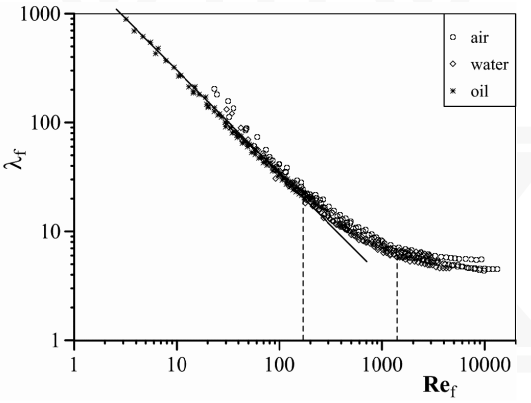

Fig. 5. Changes in friction factor as a function of Reynolds for flow of air, water and oil

The nature of changes in the two-phase flow pressure drop $(\Delta P/\Delta L)_{2f}$ is presented in Figure 6 as shown by the example of air-water flow through foam 40 PPI. Two-phase flow pressure drops are determined by phase velocity and they increase monotonically with increasing velocity, both for air w_a and water w_w.

The only departure is a sudden decrease in the value of pressure drops observed for a series of points for water flow with a velocity of 0.061 m/s. Apparently, the ungrounded decrease in the flow pressure drops despite the fact that the increase in air velocity is related to a change in the flow pattern – from plug flow to stratified flow.

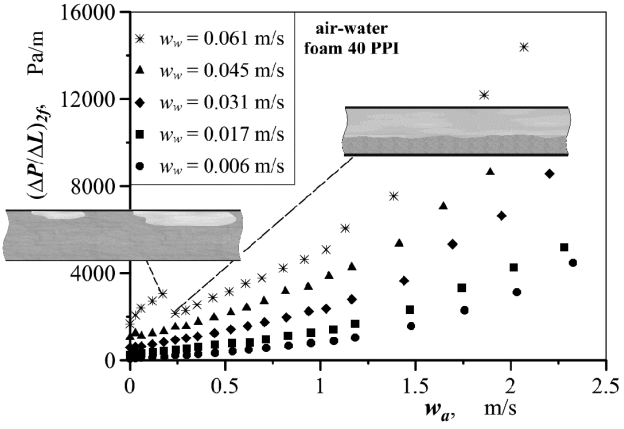

Fig. 6. Character of changes of pressure drops in air-water flow, with pressure drop reduction effect

Air-water flow occurred mainly as a stratified flow. For small streams of air introduced into the channel, a plug flow was also observed. For air-oil flow, apart from stratified and plug flow, semislug and slug flow patterns were also observed. The greater variety of air-oil flow patterns results in more irregular curve of changes in a pressure drop for this flow, especially for flows with relatively high oil velocity, when semislug and slug flow were observed in the channel.

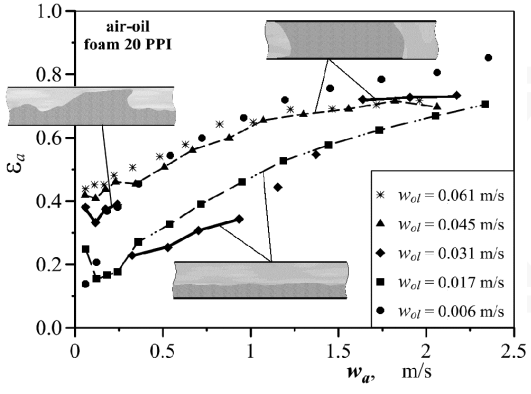

Fig. 7. Effect of phase velocity and flow pattern on value of air void fraction, in flow with oil

Flow patterns also strongly affect values of void fractions of the phases. As shown in Fig. 7, when the type of the flow changes, there is a step change in the air void fraction.

The types of flow patterns formed in the channel packed with open-cell metal foam are determined by mutual relations of fluid velocity and their properties. There was no effect of foam geometric parameters on gas–liquid flow patterns found. In the analogical flow conditions, i.e. at the same phase velocity and fractions, identical flow patterns were observed for all of the foams (for a specific mixture of gas and liquid). It is also worth noting that foam

does not cause greater phase dispersion than flow through an empty channel. Flow patterns in the channels packed with foam correspond to flow patterns occurring for a two-phase mixture flow through empty channels.

The heat transfer analysis was based on changes measured in the temperatures of the fluid and channel walls at the flow route, and heat balance in the heated part of the measurement section of the channel.

In the single-phase flow, in order to increase the fluid temperature from a value at the beginning of the heated channel section (cross-section I in Fig. 2) to a temperature at the section outlet (cross-section IV), a heat transfer rate Q_f is required,

$$Q_f = G_f \cdot \left(i_{f,\mathrm{IV}} - i_{f,\mathrm{I}} \right) \tag{4}$$

where:

G_f – fluid mass flow,

$i_{f,\mathrm{I}}$, $i_{f,\mathrm{IV}}$ – fluid enthalpy at the beginning and end of the measurement section.

In the two phase flow, heat transferred between the heated channel and air-liquid mixture has a value equal to the total of heat transfer rates to both fluids,

$$Q_{2F} = Q_a + Q_L \,, L \equiv w, ol \tag{5}$$

Value of fluid enthalpies was determined for average temperatures in the considered channel cross-sections (I and IV). For air enthalpy, a steam contained in the air was taken into account. Air humidity was measured upstream of the measurement channel. For the two-phase air-water flow, due to the need of accounting for latent heat of water vaporisation, air enthalpy was calculated for the assumed saturated state.

The calculated heat transfer rate and Newton equation allow for the determination of heat transfer coefficient from the channel wall to the fluid α_f (α_{2f} in two-phase flow),

$$\alpha_{f(2f)} = \frac{Q_{f(2f)}}{F_b \cdot \left(\overline{t}_b - \overline{t}_f \right)_m} \tag{6}$$

where:

F_b – internal surface area of wall of the heated channel section.

Due to the changing temperatures of the fluid and the wall at the flow path, value of expression $\left(\overline{t}_b - \overline{t}_f \right)_m$ was determined by approximate integration of differences of these temperatures,

$$\left(\overline{t}_b - \overline{t}_f \right)_m = \frac{1}{L_{\mathrm{VI}} - L_{\mathrm{I}}} \int_{L_1}^{L_{\mathrm{IV}}} \left(\overline{t}_b - \overline{t}_f \right) dL \tag{7}$$

Temperatures of the wall $\overline{t}_b$ and the fluid $\overline{t}_f$ were assumed as average values from all the thermocouples located in the wall (12 pcs) and inside the channel (20 pcs) located at four equidistant channel lengths (Figure 2 – cross-sections I, II, III and IV).

For all three fluids, the heat transfer coefficient in the single-phase flow shows a similar dependency on the flow conditions and parameters of the foam in the channel. Figure 8 presents an example of such behaviour of α recorded for the heating of water. The heat transfer coefficient increases with the increase of the fluid velocity. Moreover, for the same water velocity, α_w has different values for channels packed with different foams. This is probably due to differences in the foam structures and their thermal conductivity. The lowest values of the heat transfer coefficient were reported for flow through foam 30 PPI. Taking into account foam specific surface area, which next to channel internal surface area, is a "component" of heat transfer surface, coefficient α_w in flow through foam 30 PPI shall value greater than for flow through foam 20 PPI, which having larger cells, have a lower specific surface area. The behaviour observed in the studies is opposite. It shows that in the channels packed with foam, heat transfer occurs to a large extent between the channel wall and the fluid.

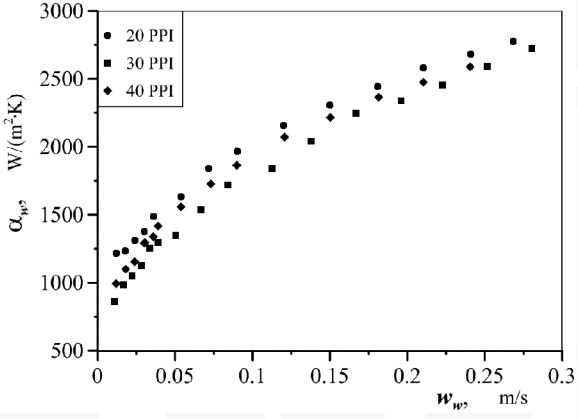

Fig. 8. Heat transfer coefficient for water flow through channels packed with various aluminium foams

The transfer coefficient for flow through foam 40 PPI has intermediate values – between values corresponding to flow through foams 20 and 30 PPI. The foam 40 PPI is geometrically similar to foam 30 PPI (similar cell and pore sizes), but it has significantly higher thermal conductivity of the skeleton k_s equal 189 W/(m·K), while k_s = 150.4 W/(m·K) for foams 20 PPI and 30 PPI. Taking into consideration the fact that part of the heat is transferred from wall to foam and then through it to the fluid, various values of thermal conductivity of the foam skeleton undoubtedly have an effect on obtaining higher values of the heat transfer coefficient for flow through foam 40 PPI, in comparison to foam 30 PPI. Results of heat conduction in the foam-fluid system are described in the paper [4].

The value of the heat transfer coefficient for the two-phase flow is greater than for the single-phase flow. For all the cases of the flow, i.e. both for air-water flow and air-oil flow through all three foams, the heat transfer rate increases with an increase in the velocity of each phase. However, liquid has greater effect on the value of α_{2f} as shown in Figure 9. Ten-fold increase in water velocity (from 0.006 to 0.061 m/s) causes approx. two-fold increase

of heat transfer coefficient. While multiple increases in the air velocity causes only a small (several percent) increase in the value of α_{2f}. Analogical behaviour in changes of heat transfer coefficient was observed for the air-oil flow.

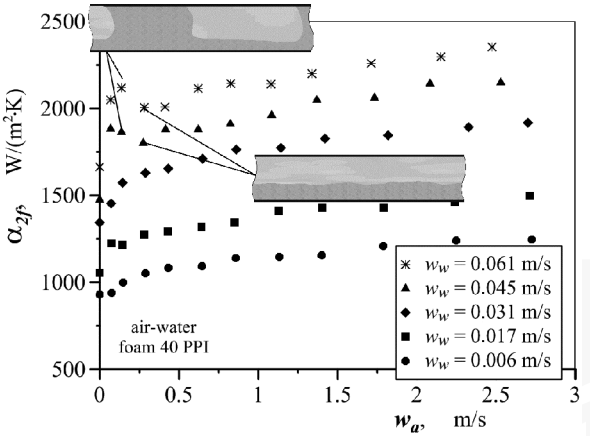

Fig. 9. Heat transfer coefficient for air-water flow for various fluid velocities

Under the conditions of changing flow patterns, some departures from the tendency of an increase in the heat transfer coefficient with an increase in the fluid velocities can be observed. However, the impact of patterns on the heat transfer rate is not as pronounced as for pressure drops and phase fractions and it points out only for air-water flow, when flow pattern changes from plug to stratified one. Under the same conditions, the greater pressure drop reduction effects were observed for the two-phase flow and step changes of void fraction of phases.

Just as for the single-phase flow, the highest values of heat transfer coefficient α_{2f} were reported for flow through foam 20 PPI and the lowest for flow through foam 30 PPI.

4. Summary

Open-cell metal foam may be used in the construction of various process equipment. There are high expectations regarding the application of foams in heat and mass exchangers, where they can be used as structural packing. In such application, it is necessary to identify factors determining pressure drops and the heat transfer in the space packed with metal foams. Results of own experimental results in that scope indicate that fluid pressure drops through channels packed with aluminium alloy foams depend on fluid velocity and fluid properties, foam porosity, cell size and shape of the cellular skeleton.

Foam geometric parameters to a smaller extent affect the heat transfer rate. Nevertheless, the heat transfer coefficient for heating the fluids in channels packed with foams under the same flow conditions has different values depending on the foam the fluid is pumped through.

These differences are as high as 20% (under conditions of the executed tests). Moreover, an effect of the foam skeleton thermal conductivity on the heat transfer between the fluid and the wall channel can be also observed.

Two-phase flow pressure drops depend mainly on flow hydrodynamic conditions, including flow patterns. In the channels filled with aluminium foams, flow patterns typical for empty channels occur. The following four basic flow patterns may be distinguished among the patterns observed in the studies: plug, semislug, slug and stratified flow patterns. The type of the formed flow patterns is determined solely by flow conditions (velocities, properties and void fractions of phases). There was no effect of foam geometric parameters on the flow patterns found.

Changes in the flow patterns are often accompanied by sudden, reaching dozens of percents, changes of values of $(\Delta P/\Delta P)_{2f}$ and ε_f. The effect of the flow patterns on value of the heat transfer coefficient in the two-phase gas–liquid flow is less pronounced.

References

[1] Boomsma K., Poulikakos D., Zwick F., *Metal foams as compact high performance heat exchangers*, Mechanics of Materials, 35, 2003, 1161–1176.

[2] Cha J.S., Ghiaasiaan S.M., Kirkconnell C.S., *Longitudinal hydraulic resistance Parameters of cryocooler and stirling Regenerators in periodic flow*, Advances in Cryogenic Engineering: Transactions of the Cryogenic Engineering Conference – CEC, 53, 2008, 259–266.

[3] Cookson E.J., Floyd D.E., Shih A.J., *Design, manufacture, and analysis of metal foam electrical resistance heather*, Int. J. Mechanical Sciences, 48, 2006, 1314–1322.

[4] Dyga R., Płaczek M., *Heat transfer through metal foam–fluid system*, Experimental Thermal and Fluid Science, Vol. 65, 2015, 1–12.

[5] Dyga R., Płaczek M., *Przepuszczalność i współczynnik inercji pian aluminiowych o komórkach otwartych*, Inżynieria i Aparatura Chemiczna, 4, 2013, 300–301.

[6] Hu H., Zhu Y., Ding G, Sun S., *Effect of oil on two-phase pressure drop of refrigerant flow boiling inside circular tubes filled with metal foam*, International Journal of Refrigeration, 36, 2013, 516–526.

[7] Incera Garrido G., Patcas F.C., Lang S., Kraushaar-Czarnetzki B., *Mass transfer and pressure drop in ceramic foams: Adescription for differentporesizesand porosities*, Chemical Engineering Science, Vol. 63, 2008, 5202–5217.

[8] Ji W.-T., Qu Z.-G., Li Z.-Y., Guo J.-F., Zhang D.-C., Tao W.-Q., P*ool boiling heat transfer of R134a on single horizontal tube surfaces sintered with open-celled copper foam*, International Journal of Thermal Sciences, 50, 2011, 2248–2255.

[9] Kamath P.M., Balaji C., Venkateshan S.P., *Experimental investigation of flow assisted mixed convection in high porosity foams in vertical channels*, International Journal of Heat and Mass Transfer, 54, 2011, 5231–5241.

[10] Lévêque J., Rouzineau D., Prévost M., Meyer M., *Hydrodynamic and mass transfer efficiency of ceramic foam packing applied to distillation*, Chemical Engineering Science, 64, 2009, 2607–2616.

[11] Ozmat B., Leyda B., Benson B., *Thermal applications of open cell metal foams*, Character and Manufacturing Processes, Vol. 19(5), 2004, 839–862.
[12] Pangarkar K.,Schildhauer T.J., van Ommen J.R., Nijenhuis J., Moulijn J.A., Kapteijn F., *Heat transport in structured packings with co-current downflow of gas and liquid,* Chemical Engineering Science, 65, 2010, 420–426.
[13] Paserin V., Marcuson S., Shu J., Wilkinson D.S., *The chemical vapor deposition technique for Inco nickel foam production–manufacturing benefits and potential applications*, Cellular Metalls and Foaming Technology, 2003, ftp://207.102.129.71/Richard/stuff/Ni-MH/metfoam_03_paper.pdf (access: 17.11.2013).
[14] Ribeiro G.B., Barbosa Jr.J.R., *Comparison of metal foam and louvered fins as air-side heat transfer enhancement media for miniaturized condensers*, Applied Thermal Engineering, 51, 2013, 334–337.
[15] Stemmet C.P., Meeuwse M., van der Schaaf J., Kuster B.F.M., Schouten J.C., *Gas–liquid mass transfer and axial dispersion in solid foam packings*, Chemical Engineering Science, 62, 2007, 5444–5450.
[16] Sertkaya A.A., Altınısık K., Dincer K., *Experimental investigation of thermal performance of aluminum finned heat exchangers and open-cell aluminum foam heat exchangers*, Experimental Thermal and Fluid Science, 36, 2012, 86–92.
[17] Tadrist L., Miscevic M., Rahli O., Topin F., *About the use of fibrous materials in compact heat exchangers*, Experimental Thermal and Fluid Science, 28, 2004, 193–199.
[18] Tian Y., Zhao C.Y., *Thermal and exergetic analysis of Metal Foam-enhanced Cascaded Thermal Energy Storage (MF-CTES)*, International Journal of Heat and Mass Transfer, 58, 2013, 86–96.
[19] Tschentscher R., Schubert M., Bieberle A., Nijhuis T.A., van der Schaaf J., Hampel U., Schouten J.C., *Tomography measurements of gas holdup in rotating foam reactors with Newtonian, non-Newtonian and foaming liquids*, Chemical Engineering Science, 66, 2011, 3317–3327.
[20] Vadwala P.H., *Thermal Energy Storage in Copper Foams filled with Paraffin Wax*, Master of Applied Science, Mechanical & Industrial Engineering University of Toronto, 2011.
[21] Wang K., Ju Y.L., Lu X.S., Gu A.Z., *On the performance of copper foaming metal in the heat exchangers of pulse tube refrigerator*, Cryogenics, 47, 2007, 19–24.
[22] Wang P., Liu D.Y., Xu C., *Numerical study of heat transfer enhancement in the receiver tube of direct steam generation with parabolic trough by inserting metal foams*, Applied Energy, 102, 2013, 449–460.
[23] Xu Z.G., Qu Z.G., Zhao C.Y., Tao W.Q., *Pool boiling heat transfer on open-celled metallic foam sintered surface under saturation condition*, International Journal of Heat and Mass Transfer, 54, 2011, 3856–3867.